IEEE Access
Multidisciplinary : Rapid Review : Open Access Journal

Received January 20, 2021, accepted January 27, 2021, date of publication February 1, 2021, date of current version March 18, 2021.

Digital Object Identifier 10.1109/ACCESS.2021.3056051

Performance of Cell-Free Massive MIMO With Joint User Clustering and Access Point Selection

RUI WANG[1,2], MIN SHEN[1], YUN HE[1], (Graduate Student Member, IEEE), AND XIANGYAN LIU[1]

[1]School of Communication and Information Engineering, Chongqing University of Posts and Telecommunications, Chongqing 400065, China
[2]School of Physics and Electronic Engineering, Yuxi Normal University, Yunnan 653100, China

Corresponding author: Min Shen (shenmin@cqupt.edu.cn)

This work was supported in part by the Joint Special Project for Basic Research of Yunnan Provincial Local Universities (part) (Youth Project) under Grant 2018FH001-120, and in part by the Science and Technology Research Project of Chongqing Education Commission under Grant KJQN201800618.

ABSTRACT We consider an uplink cell-free massive multiple-input multiple-output (MIMO) system, in which the access points are connected to the central processing unit (CPU) through a fronthaul network. This system has the advantages of wide coverage and flexible deployment. However, the performance of this system depends on a capacity-limited fronthaul, and when the fronthaul is saturated, the quality of service will be reduced. To address this issue, we propose a joint user clustering and AP selection scheme, which can reduce the pressure on the fronthaul link while taking into account the system performance and computational complexity. We first derive a closed-form expression for the uplink spectral efficiency over Rician fading channels. Based on the derived expression, we formulate the problem of maximizing the minimum uplink spectral efficiency across all users by jointly optimizing the large-scale fading decoding (LSFD) coefficient and power control coefficient. Then, combined with the optimization results and channel estimation error, a suboptimal access point selection scheme is proposed. In addition, we propose a user clustering scheme to further reduce the complexity of the AP selection scheme. The simulation results show that the joint user clustering and access point selection scheme can reduce the system fronthaul link pressure, while the performance degrades only slightly.

INDEX TERMS Access point selection, cell-free massive MIMO, spectral efficiency, user clustering.

I. INTRODUCTION

Cell-free massive MIMO is a promising technology suitable for beyond-5G and 6G networks because of its massive connections, low latency, high speed, and high reliability [1]. It is a user-centric distributed MIMO system. In cell-free massive MIMO systems, all APs are connected and cooperate with the central processing unit through a fronthaul network to provide services for all users through time division duplex technology on the same time-frequency resources [2]. Considering the large-scale deployment of APs, cell-free massive MIMO systems have favourable propagation and channel hardening characteristics, so they have significant advantages in spectral efficiency [3]. However, the benefits of cell-free massive MIMO come at the expense of increased fronthaul capacity requirements. In addition, a capacity-constrained fronthaul link may significantly affect the system performance [4]. Bashar *et al.* [5], [6] propose the method of sending quantitative signals to reduce the burden of fronthaul links. However, the above works assume that all APs simultaneously serve all users. Such a framework is of course unrealistic and unscalable in practice.

In addition, Ngo *et al.* [7] propose that due to the capacity limitation of the fronthaul load [8] and hardware impairments [9], it is not the best choice for all APs to serve all users during the uplink and downlink data transmission stages. Therefore, AP selection is a practically feasible solution for fronthaul burden reduction [10], [11]. Currently, Ngo *et al.* [7] propose an AP selection scheme based on largest large-scale fading in which each user is served by only some nearby APs. Therefore, the AP selection algorithm in [7] cannot guarantee the superiority of system performance [12]. To optimize the system performance while performing AP selection, Boroujerdi *et al.* [13] propose an AP

The associate editor coordinating the review of this manuscript and approving it for publication was Zhen Gao.

selection scheme based on the sum-rate optimization problem. Vu *et al.* [14] optimize the energy efficiency of the system using a joint power allocation and AP selection scheme. Chien *et al.* [15] propose a downlink power minimization problem and use the results from the optimization problem to select active APs. Dong *et al.* [16] analyse an energy efficiency optimization problem involving power allocation, user association, and antenna activation and solve the problem by applying hierarchical decomposition technology and an iterative successive convex approximation algorithm, but the algorithm has high computational complexity. Therefore, it is necessary to propose an AP selection algorithm that can balance the system performance and algorithm complexity. At the same time, since a large number of APs and users are deployed in the cell-free massive MIMO system, it is not sufficient to reduce the complexity from only the AP side. the algorithmic complexity can be effectively reduced by user clustering before AP selection. Moreover, all the above studies are carried out under the Rayleigh fading channel model without considering the line-of-sight (LOS) path. However, the practical channel has Rician fading formed by the combination of the multipath signal component and the line-of-sight signal component. In [17], the authors study the AP selection strategy for cell-free massive MIMO with a Rician fading channel but do not consider user clustering and multi-antenna APs.

This paper aims to fill the above gaps in the literature. The main contributions of this work are outlined as follows:

- We derive a closed-form expressions for the uplink spectral efficiency of cell-free massive MIMO that takes into account the imperfect CSI, AP selection, LSFD coefficient, and power control. Our result is a generalization of the result in [18], in which AP selection and multiple-antenna AP were not considered.
- To reduce the pressure on the fronthaul link while taking into account the system performance. Based on the derived closed-form expression, we formulate and solve a spectral efficiency optimization problem involving access point selection, power control and the LSFD coefficient. The joint optimization problem is an integer programming problem, so the problems are separated so that each one can be simplified. First, an iterative optimization algorithm is adopted to solve the problem of maximizing the minimum spectral efficiency across all users, while the optimization variables are the LSFD coefficient and the power control coefficient. On this basis, a suboptimal access point selection algorithm based on the optimization outcome and channel estimation error is also proposed.
- We propose a user grouping scheme based on hierarchical clustering. We group users with high channel similarity into the same cluster, and users in each cluster need to perform AP selection only once. Through the joint processing of user clustering and AP selection, the proposed algorithm reduces the computational complexity of the system while ensuring good system performance.

This article is organized as follows: In the second section, we describe the system model and spectral efficiency. In the third section, we introduce the LSFD coefficient and power distribution optimization schemes. Section IV discusses the user clustering and access point selection schemes. The fifth section provides numerical results and discussion, and the sixth section summarizes the article. Table 1 lists the notation and symbols used throughout the paper.

TABLE 1. Notation and symbols.

Notation	Definition
$(\cdot)^T, (\cdot)^H$	Transpose and conjugate transpose
$(\cdot)^*$	The complex conjugate operation
$\|\cdot\|_F$,	Frobenius norms
$E\{\cdot\}$	Expectation value
$\mathcal{N}_{\mathbb{C}}(\cdot,\cdot)$	Circularly symmetric complex Gaussian distribution

II. SYSTEM MODEL AND SPECTRAL EFFICIENCY

The layout of the cell-free massive MIMO system is shown in Fig. 1. M APs equipped with N antennas and K users equipped with a single antenna are randomly distributed in the coverage area. The APs and the CPU are connected through the fronthaul link.

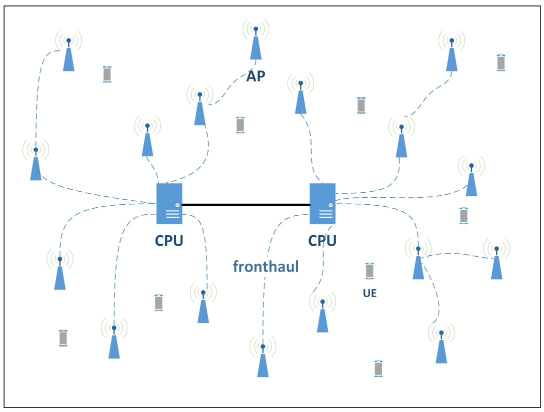

FIGURE 1. Network deployment of a cell-free massive MIMO system.

A. SYSTEM MODEL

1) PROPAGATION MODEL

We consider a Rician fading channel composed of line-of-sight and multipath components. The channel $\boldsymbol{h}_{mk} \in \mathbb{C}^{N\times 1}$ from the mth AP to the kth user can be modeled as:

$$\boldsymbol{h}_{mk} = e^{j\theta_{mk}}\bar{\boldsymbol{h}}_{mk} + \tilde{\boldsymbol{h}}_{mk}, \tag{1}$$

where $\bar{\boldsymbol{h}}_{mk}$ represents the LoS component and $\theta_{mk} \sim \mathcal{U}[-\pi,\pi]$ is the phase shift. $\tilde{\boldsymbol{h}}_{mk} \sim \mathcal{N}_{\mathbb{C}}(\mathbf{0}_N, \beta_{mk}\boldsymbol{I}_N)$. β_{mk} is a large-scale fading coefficient that takes into account path loss and shadowing. We model the LoS component $\bar{\boldsymbol{h}}_{mk}$ and β_{mk} as

$$\bar{\boldsymbol{h}}_{mk} = \Delta_{mk}\left[1, \mathrm{e}^{-j2\pi d\sin\varphi_{mk}}, \ldots, \mathrm{e}^{-j2\pi d(N-1)\sin\varphi_{mk}}\right]^T, \tag{2}$$

$$\Delta_{mk} = \sqrt{\frac{\kappa_{mk} PL_{mk}}{\kappa_{mk}+1}}, \tag{3}$$

and

$$\beta_{mk} = \frac{1}{\kappa_{mk}+1}\mathrm{PL}_{mk}, \tag{4}$$

where $d = 0.5$ is the antenna spacing coefficient and $\varphi_{mk} \sim \mathscr{U}[-\pi,\pi]$ is the arrival angle at the kth user seen from the mth AP. PL_{mk} represents the path loss (in dB). κ_{mk} is the Rician factor. The system adopts the time division duplex (TDD) mode to complete the transmission between users and APs. Each coherent time interval of length τ_c samples is composed of three stages: uplink training, uplink data transmission and downlink data transmission.

2) CHANNEL ESTIMATION

As in [19], in the uplink training phase, all users simultaneously send the same or mutually orthogonal pilot sequences to all APs for channel estimation. The pilot sequence assigned to each user is $\boldsymbol{\varphi}_k \in \mathbb{C}^{\tau}$, and it satisfies $\|\boldsymbol{\varphi}_k\|^2 = \tau$. We assume that the length of the pilot sequence is less than the number of users K. We define the set $\mathscr{P}_k$ as the set of users who use the same pilot as user k. The power of the pilot sequence is ρ_{p}. Then, the pilot signal $\boldsymbol{Y}_{p,m} \in \mathbb{C}^{N\times\tau}$ received at AP m is

$$\boldsymbol{Y}_{p,m} = \sqrt{\rho_{\mathrm{p}}}\sum_{k=1}^{K} \boldsymbol{h}_{mk}\boldsymbol{\varphi}_k^T + \boldsymbol{N}_{p,m}, \tag{5}$$

where $\boldsymbol{N}_{p,m} \in \mathbb{C}^{N\times\tau}$ is an additive noise matrix, and its elements are i.i.d. $\mathscr{N}_{\mathbb{C}}\left(0,\sigma^2\right)$ random variables. Then, we multiply $\boldsymbol{Y}_{p,m}$ by $\frac{\boldsymbol{\varphi}_k^*}{\sqrt{\tau}}$ to obtain

$$\boldsymbol{y}_{mk} = \sqrt{\rho_p \tau}\sum_{l\in\mathscr{P}_k} \boldsymbol{h}_{ml} + \frac{\boldsymbol{N}_{p,m}\boldsymbol{\varphi}_k^*}{\sqrt{\tau}}. \tag{6}$$

Compared with the LMMSE channel estimation algorithm, the MMSE channel estimation algorithm has better estimation performance. However, the MMSE channel estimation algorithm needs to know the phase shifts of the LOS components, which is not widely applicable. Moreover, since we do not have a linear Gaussian signal model, it is not easy to derive the MMSE estimator under an unknown phase shift. In this paper, we use the method described in [20] to perform LMMSE channel estimation. Thus, the estimate of $\boldsymbol{h}_{mk}$ based on (6) is given by

$$\hat{\boldsymbol{h}}_{mk} = \sqrt{\rho_p\tau}\boldsymbol{R}_{mk}\boldsymbol{\Phi}_{mk}^{-1}\boldsymbol{y}_{mk}, \tag{7}$$

where $\boldsymbol{R}_{mk} \triangleq \mathbb{E}\left\{\boldsymbol{h}_{mk}\boldsymbol{h}_{mk}^H\right\} = \bar{\boldsymbol{h}}_{mk}\bar{\boldsymbol{h}}_{mk}^H + \beta_{mk}\boldsymbol{I}_N$ and $\boldsymbol{\Phi}_{mk} = \mathbb{E}\left\{\boldsymbol{y}_{mk}\boldsymbol{y}_{mk}^H\right\} = \rho_p\tau\sum_{l\in\mathscr{P}_k}\boldsymbol{R}_{ml} + \sigma^2\boldsymbol{I}_N$.

The channel estimate $\hat{\boldsymbol{h}}_{mk}$ and the estimation error $\boldsymbol{e}_{mk} = \boldsymbol{h}_{mk} - \hat{\boldsymbol{h}}_{mk}$ have zero mean and the covariance matrices

$$\hat{\boldsymbol{R}}_{mk} \triangleq \mathbb{E}\left\{\hat{\boldsymbol{h}}_{mk}\hat{\boldsymbol{h}}_{mk}^H\right\} = \rho_p\tau\boldsymbol{R}_{mk}\boldsymbol{\Phi}_{mk}^{-1}\boldsymbol{R}_{mk}, \tag{8}$$

$$\boldsymbol{C}_{mk} \triangleq \mathbb{E}\left\{\boldsymbol{e}_{mk}\boldsymbol{e}_{mk}^H\right\} = \boldsymbol{R}_{mk} - \rho_p\tau\boldsymbol{R}_{mk}\boldsymbol{\Phi}_{mk}^{-1}\boldsymbol{R}_{mk}. \tag{9}$$

The channel estimate error $\boldsymbol{e}_{mk}$ includes N components. The mean-squared error of the lth component is denoted as Var_{mlk} and given by

$$\begin{aligned} Var_{mlk} &\triangleq \mathbb{E}\left\{|[\boldsymbol{e}_{mk}]_l|^2\right\} \\ &= (\beta_{mk} + \left[\bar{\boldsymbol{h}}_{mk}\right]_l^2) \\ &\quad - \frac{\tau\rho_{\mathrm{p}}(\beta_{mk}+\left[\bar{\boldsymbol{h}}_{mk}\right]_l^2)^2}{\rho_p\tau\sum_{i\in\mathscr{P}_k}(\beta_{mi}+\left[\bar{\boldsymbol{h}}_{mi}\right]_l^2)+\sigma^2}, \end{aligned} \tag{10}$$

where $[\boldsymbol{e}_{mk}]_l$ and $\left[\bar{\boldsymbol{h}}_{mk}\right]_l$ are the lth elements of the vectors $\boldsymbol{e}_{mk}$ and $\bar{\boldsymbol{h}}_{mk}$.

B. SPECTRAL EFFICIENCY

In the uplink information transmission phase, we define a set of AP selection diagonal matrices $\boldsymbol{D}_k$, where $\boldsymbol{D}_k = \mathrm{diag}\left(d_{1\,k},\ldots,d_{Mk}\right)$. More precisely, the mth diagonal element of $\mathbf{D}_k$ is 1 if the mth AP is allowed to decode signals from user k, and it is 0 otherwise. Let s_k denote the symbol of the kth user with $\mathbb{E}\left\{|s_k|^2\right\} = 1$. The signal received at the mth AP is given by

$$\boldsymbol{z}_m^u = \sqrt{\rho_u}\sum_{k=1}^{K}\sqrt{p_k}\boldsymbol{h}_{mk}s_k + \boldsymbol{n}_m^u, \quad m = 1,\ldots,M, \tag{11}$$

where p_k, $0 \le p_k \le 1$, is the power control coefficient, ρ_u denotes the normalized uplink SNR, and $\boldsymbol{n}_m^u \sim \mathscr{N}_{\mathbb{C}}\left(\mathbf{0}_N,\sigma^2\mathbf{I}_N\right)$. The signal is decoded in two layers. In the first layer of decoding, the mth AP locally detects the useful signal of the kth user through the conjugate transpose of its estimated channel, $\hat{\boldsymbol{h}}_{mk}^H$. Thus, the first-layer decoded signal at the mth AP is

$$\tilde{r}_{mk} = \hat{\boldsymbol{h}}_{mk}^H\boldsymbol{z}_m^u = \sqrt{\rho_u}\sum_{k'=1}^{K}\sqrt{p_{k'}}\hat{\boldsymbol{h}}_{mk}^H\boldsymbol{h}_{mk'}s_{k'} + \hat{\boldsymbol{h}}_{mk}^H\boldsymbol{n}_m^u. \tag{12}$$

The CPU receives the first-layer decoded signal and performs the second-layer decoding by computing the large-scale fading decoding (LSFD) weighted signal [21] involving a subset of the APs. The second-layer decoded signal received and processed at the CPU is

$$\begin{aligned} \hat{r}_k &= \sum_{m=1}^{M} d_{mk}\alpha_{mk}^*\hat{\boldsymbol{h}}_{mk}^H\boldsymbol{z}_m^u \\ &= \sum_{m=1}^{M}\sqrt{p_k\rho_u}d_{mk}\alpha_{mk}^*\hat{\boldsymbol{h}}_{mk}^H\boldsymbol{h}_{mk}s_k \\ &\quad + \sum_{m=1}^{M}\sum_{\substack{k'=1\\k'\neq k}}^{K}\sqrt{p_{k'}\rho_u}d_{mk}\alpha_{mk}^*\hat{\boldsymbol{h}}_{mk}^H\boldsymbol{h}_{mk'}s_{k'} \\ &\quad + \sum_{m=1}^{M} d_{mk}\alpha_{mk}^*\hat{\boldsymbol{h}}_{mk}^H\boldsymbol{n}_m^u, \end{aligned} \tag{13}$$

where α_{mk} is the complex LSFD coefficient for AP m and user k. The inter-user interference is reduced by using the

LSFD coefficient. The AP selection coefficient d_{mk} reduces the burden of the fronthaul link by allowing only some of the APs to participate in signal detection. The lower bound on the uplink ergodic SE for the kth user with the LSFD and AP selection coefficient is

$$SE_k = \frac{\tau_u}{\tau_c} \log_2 (1 + SINR_k), \tag{14}$$

$$SINR_k = \frac{|T_1|^2}{\mathbb{E}\left\{|T_2|^2\right\} + \sum_{k' \neq k}^{K} \mathbb{E}\left\{|T_3|^2\right\} + \mathbb{E}\left\{|T_4|^2\right\}}, \tag{15}$$

where T_1, T_2, T_3, and T_4 represent the strength of the desired signal, the beamforming gain uncertainty, the interference from user k', and the noise. Due to the properties of LMMSE estimation, The channel estimate $\hat{\boldsymbol{h}}_{mk}$ and the channel estimation error $\boldsymbol{e}_{mk}$ are uncorrelated. Thus, we can get

$$\begin{aligned} T_1 &= \sqrt{p_k \rho_u} \sum_{m=1}^{M} d_{mk} \alpha_{mk}^* \mathbb{E}\left\{\hat{\boldsymbol{h}}_{mk}^H \boldsymbol{h}_{mk}\right\} \\ &= \sqrt{p_k \rho_u} \sum_{m=1}^{M} d_{mk} \alpha_{mk}^* \mathbb{E}\left\{\hat{\boldsymbol{h}}_{mk}^H \hat{\boldsymbol{h}}_{mk}\right\}, \end{aligned} \tag{16}$$

$$\begin{aligned} T_2 &= \sqrt{p_k \rho_u} \sum_{m=1}^{M} d_{mk} \alpha_{mk}^* \left(\hat{\boldsymbol{h}}_{mk}^H \boldsymbol{h}_{mk} - \mathbb{E}\left\{\hat{\boldsymbol{h}}_{mk}^H \hat{\boldsymbol{h}}_{mk}\right\}\right) \\ &= \sqrt{p_k \rho_u} \sum_{m=1}^{M} d_{mk} \alpha_{mk}^* \left(\hat{\boldsymbol{h}}_{mk}^H \left(\hat{\boldsymbol{h}}_{mk} + \boldsymbol{e}_{mk}\right)\right) - T_1, \end{aligned} \tag{17}$$

$$\begin{aligned} T_3 &= \sqrt{p_{k'} \rho_u} \sum_{m=1}^{M} d_{mk} \alpha_{mk}^* \hat{\boldsymbol{h}}_{mk}^H \boldsymbol{h}_{mk'} \\ &= \sqrt{p_{k'} \rho_u} \sum_{m=1}^{M} d_{mk} \alpha_{mk}^* \left(\hat{\boldsymbol{h}}_{mk}^H \left(\hat{\boldsymbol{h}}_{mk'} + \boldsymbol{e}_{mk'}\right)\right), \end{aligned} \tag{18}$$

$$T_4 = \sum_{m=1}^{M} d_{mk} \alpha_{mk}^* \hat{\boldsymbol{h}}_{mk}^H \boldsymbol{n}_m^u. \tag{19}$$

The effective SINR of user k in (15) with the LSFD and AP selection coefficient can be rewritten as

$$SINR_k = \frac{p_k \rho_u \left|\boldsymbol{u}_k^H \boldsymbol{v}_k\right|^2}{\boldsymbol{u}_k^H \left(\sum_{k'=1}^{K} p_{k'} \rho_u \boldsymbol{W}_{kk'}\right) \boldsymbol{u}_k - p_k \rho_u \left|\boldsymbol{u}_k^H \boldsymbol{v}_k\right|^2 + \boldsymbol{u}_k^H \boldsymbol{X}_k \boldsymbol{u}_k}, \tag{20}$$

where $\boldsymbol{u}_k = \operatorname{diag}(\boldsymbol{A}_k \boldsymbol{D}_k)$, $\mathbf{A}_k = \operatorname{diag}(\alpha_{1\,k}, \ldots, \alpha_{Mk})$, and $u_{mk} = d_{mk} \alpha_{mk}$. $\boldsymbol{v}_k \triangleq \left[v_{1k} \ldots v_{Mk}\right]^T$. $\boldsymbol{X}_k$ is a diagonal matrix, and its mth diagonal element is $x_{mk} = \sigma^2 \operatorname{tr}\left(\hat{\mathbf{R}}_{mk}\right)$. $w_{kk'}^{mm'}$ is the (m, m')th element of the matrix $\boldsymbol{W}_{kk'}$. The elements of $\boldsymbol{v}_k$ and $\boldsymbol{W}_{kk'}$ are given as

$$\begin{aligned} v_{mk} &= \mathbb{E}\left\{\hat{\boldsymbol{h}}_{m,k}^H \hat{\boldsymbol{h}}_{m,k}\right\} \\ &= \tau \rho_p \overline{\boldsymbol{h}}_{mk}^H \boldsymbol{\Phi}_{mk}^{-1} \boldsymbol{R}_{mk} \overline{\boldsymbol{h}}_{mk} + \tau \rho_p \beta_{mk} \operatorname{tr}\left(\boldsymbol{\Phi}_{mk}^{-1} \boldsymbol{R}_{mk}\right), \end{aligned} \tag{21}$$

$$\begin{aligned} w_{kk'}^{mm} &= \mathbb{E}\left\{\hat{\boldsymbol{h}}_{mk}^H \boldsymbol{h}_{mk'} \boldsymbol{h}_{mk'}^H \hat{\boldsymbol{h}}_{mk}\right\} \\ &= \mathbb{E}\left\{\hat{\boldsymbol{h}}_{mk}^H \left(\hat{\boldsymbol{h}}_{mk'} + \boldsymbol{e}_{mk'}\right) \left(\hat{\boldsymbol{h}}_{mk'} + \boldsymbol{e}_{mk'}\right)^H \hat{\boldsymbol{h}}_{mk}\right\} \\ &= \begin{cases} 2\tau^2 \rho_p^2 \beta_{mk'} \Re\left\{\overline{\boldsymbol{h}}_{mk'}^H \boldsymbol{\Phi}_{mk}^{-1} \boldsymbol{R}_{mk} \overline{\boldsymbol{h}}_{mk'} \operatorname{tr}\left(\boldsymbol{R}_{mk} \boldsymbol{\Phi}_{mk}^{-1}\right)\right\} & \\ +\tau^2 \rho_p^2 \beta_{mk'}^2 \left|\operatorname{tr}\left(\boldsymbol{\Phi}_{mk}^{-1} \boldsymbol{R}_{mk}\right)\right|^2 & \\ +\tau \rho_p \operatorname{tr}\left(\boldsymbol{\Phi}_{mk}^{-1} \boldsymbol{R}_{mk} \boldsymbol{R}_{mk'} \boldsymbol{R}_{mk}\right) & k' \in \mathscr{P}_k \\ \operatorname{tr}\left(\hat{\boldsymbol{R}}_{mk} \boldsymbol{R}_{mk'}\right) & k' \notin \mathscr{P}_k. \end{cases} \end{aligned} \tag{22}$$

To reduce the pressure of the fronthaul link while considering the spectral efficiency of the system, we investigate a joint optimization problem involving access point selection, power control, and the LSFD coefficient. However, the joint optimization problem involves access point selection and is an integer optimization problem, which increases the complexity of system processing. To reduce the complexity of system optimization processing, we separate the optimization problems. First, we establish the maximizing minimum spectral efficiency optimization problem with the power control coefficient and the LSFD coefficient as the optimization variables. Then, a suboptimal access point selection algorithm based on the optimization results is proposed. In Section III, the maximizing minimum spectral efficiency optimization problem is solved. Access point selection is proposed in Section IV.

III. LSFD COEFFICIENT AND POWER OPTIMIZATION

Based on the previous analysis, we summarize the joint optimization problem for the LSFD coefficient and power control coefficient as follows:

$$\begin{aligned} P: \quad & \max_{\{p, \boldsymbol{\alpha}_k\}} \min_{k=1,\cdots,K} SINR_k \\ & \text{subject to } 0 \le p_k \le 1, k = 1, \ldots, K, \\ & \qquad \|\boldsymbol{\alpha}_k\|^2 \le 1, k = 1, \ldots, K, \end{aligned} \tag{24}$$

where $SINR_k$ is from (20) and $\boldsymbol{\alpha}_k = \left[\alpha_{1,k}, \ldots, \alpha_{M,k},\right]^T$, $p \triangleq (p_k)_{k=1,\ldots,K}$. Problem (24) can be equivalently expressed as

$$\begin{aligned} P: \quad & \max_{\{p, \boldsymbol{\alpha}_k\}, t} t \\ & \text{subject to } SINR_k(p, \boldsymbol{\alpha}_k) \ge t, k = 1, \ldots, K, \\ & \qquad 0 \le p_k \le 1, k = 1, \ldots, K, \\ & \qquad \|\boldsymbol{\alpha}_k\|^2 \le 1, k = 1, \ldots, K. \end{aligned} \tag{25}$$

The above joint optimization problem is nonconvex. To solve this problem, we can decouple it and use iterative optimization to solve it. As long as one of the optimization parameters of p_k and $\boldsymbol{\alpha}_k$ is regarded as fixed, the optimization problem can be converted into a convex optimization problem. In the initial phase, we set the AP selection matrix $\boldsymbol{D}_k$ as the identity matrix. We first fix the LSFD coefficient, and then the optimization problem of the power control coefficient can be written as follows:

$$\begin{aligned} P_1: \ & \max_{\{p\},t} t \\ & \text{subject to } SINR_k(p) \geq t, \quad k = 1, \ldots, K, \\ & 0 \leq p_k \leq 1, \quad k = 1, \ldots, K. \end{aligned} \tag{26}$$

If t is a given value, all inequalities in (26) are linear, so (26) is a quasi-linear problem. Therefore, the bisection method can effectively solve problem (26).

Next, we fix the power control coefficient, the optimization problem of the LSDF coefficient can be written as follows:

$$\begin{aligned} P_2: \ & \max_{\{\boldsymbol{\alpha}_k\}} \min_{k=1,\cdots,K} SINR_k \\ & \text{subject to } \|\boldsymbol{\alpha}_k\|^2 \leq 1, k = 1, \ldots, K. \end{aligned} \tag{27}$$

To obtain the optimal solution of the LSFD coefficient, we rewrite the SINR as:

$$SINR_k = \frac{p_k \rho_u \left|\boldsymbol{\alpha}_k^H \boldsymbol{v}_k\right|^2}{\boldsymbol{\alpha}_k^H \left(\sum_{k'=1}^{K} p_{k'} \rho_u \boldsymbol{W}_{kk'} - \rho_u p_k \boldsymbol{v}_k \boldsymbol{v}_k^H + \boldsymbol{X}_k\right) \boldsymbol{\alpha}_k}. \tag{28}$$

Since $SINR_k$ only depends on $\boldsymbol{\alpha}_k$, we can obtain the solution of problem P_2 by solving the K optimization problems separately. Note that $\boldsymbol{\alpha}_k$ must be normalized, so $\|\boldsymbol{\alpha}_k\|^2 = 1$. The SINR expression in (28) is a generalized Rayleigh quotient with respect to $\boldsymbol{\alpha}_k$, and we apply [22] to obtain the maximizing $\boldsymbol{\alpha}_k$ as

$$\boldsymbol{\alpha}_k = \left(\sum_{k'=1}^{K} p_{k'} \rho_u \boldsymbol{W}_{kk'} - \rho_u p_k \boldsymbol{v}_k \boldsymbol{v}_k^H + \boldsymbol{X}_k\right)^{-1} \boldsymbol{v}_k. \tag{29}$$

Based on the above analysis, we summarize the joint optimization algorithm of the power control coefficient and LSFD coefficient, and the iterative optimization algorithm is shown in Algorithm 1.

Algorithm 1 Alternating Optimization for Solving (24)

1. Initialization: set the initial value of the LSFD Coefficient. Choose $t_{\min} = 0$ and $t_{\max} = t_{\text{ini}}$ as the initial values of the maximum and minimum SINRs and define the tolerance $\epsilon > 0$.
2. Set $t = \frac{t_{\min}+t_{\max}}{2}$. Solve the linear feasibility problem in (26).
3. If problem (26) is feasible and the solution is p_k^*, replace p_k with p_k^* in (24) to find the optimal LSFD coefficients $\boldsymbol{\alpha}_k^*$, and set $t_{\min} := t$. If the problem is not feasible, set $t_{\max} := t$
4. Stop if $t_{\max} - t_{\min} < \epsilon$ and set $\boldsymbol{\alpha}_k^* = \boldsymbol{\alpha}_k^* / \left\|\boldsymbol{\alpha}_k^*\right\|$. Otherwise, go to Step 2.

IV. USER CLUSTERING AND ACCESS POINT SELECTION

In this section, we propose a joint user clustering and access point selection algorithm considering both system performance and complexity.

A. USER CLUSTERING

In cell-free massive MIMO systems, traditional AP selection algorithms usually aim at maximizing the sum rate or energy efficiency [13], [16]. Although this algorithm can achieve good performance, it will significantly increase the computational complexity. Some improved fast algorithms can significantly reduce the computational complexity of AP selection without significantly affecting the system performance [12], [23]. However, the above methods consider reducing the algorithmic complexity only from the AP side. In cell-free massive MIMO systems, the numbers of users and APs are relatively large. The complexity of the AP selection algorithm is related to both the number of APs and users. Therefore, it is far from sufficient to reduce the complexity from only the AP side. For these reasons, we propose a user clustering scheme to further reduce the complexity of the AP selection algorithm. Our proposed user clustering algorithm divides users with high channel similarity into the same cluster, and users in this cluster need to select APs only once. By user clustering, the number of AP selections is reduced, thus further reducing the complexity of the AP selection algorithm as well.

The k-means and hierarchical clustering algorithms are two commonly used user clustering algorithms. The traditional k-means algorithm [24] is a classic user clustering algorithm

TABLE 2. Definition of link distance in hierarchical clustering [26].

Link method	Link method definition
single linkage	$d_{(v_i,v_j),v_q} \triangleq \min\left\{d_{v_i,v_q}, d_{v_j,v_q}\right\}$
Complete linkage	$d_{(v_i v_j),v_q} \triangleq \max\left\{d_{v_i,v_q}, d_{v_j,v_q}\right\}$
Median linkage	$d_{(v_i v_j),v_q} \triangleq \frac{1}{2} d_{v_i,v_q} + \frac{1}{2} d_{v_j,v_q} - \frac{1}{4} d_{v_i,v_j}$
Average linkage	$d_{(v,v_j),v_q} \triangleq \frac{\lvert v_i \rvert d_{v_i,v_q} + \lvert v_j \rvert d_{v_j,v_q}}{\lvert (v_i v_j) \rvert}$
Weighted average linkage	$d_{(v_i,v_j),v_q} \triangleq \frac{1}{2} d_{v_i,v_q} + \frac{1}{2} d_{v_j,v_q}$

$$\begin{aligned} w_{kk'}^{mm'} &= \mathbb{E}\left\{\hat{\boldsymbol{h}}_{mk}^H \boldsymbol{h}_{mk'} \boldsymbol{h}_{m'k'}^H \hat{\boldsymbol{h}}_{m'k}\right\} = \mathbb{E}\left\{\hat{\boldsymbol{h}}_{mk}^H \left(\hat{\boldsymbol{h}}_{mk'} + \boldsymbol{e}_{mk'}\right) \left(\hat{\boldsymbol{h}}_{m'k'} + \boldsymbol{e}_{m'k'}\right)^H \hat{\boldsymbol{h}}_{m'k}\right\} \\ &= \begin{cases} \tau^2 \rho_p^2 \left(\overline{\boldsymbol{h}}_{mk'}^H \boldsymbol{\Phi}_{mk}^{-1} \boldsymbol{R}_{mk} \overline{\boldsymbol{h}}_{mk'} + \beta_{mk'} \operatorname{tr}\left(\boldsymbol{\Phi}_{mk}^{-1} \boldsymbol{R}_{mk}\right)\right) \left(\overline{\boldsymbol{h}}_{m'k'}^H \boldsymbol{\Phi}_{m'k}^{-1} \boldsymbol{R}_{m'k} \overline{\boldsymbol{h}}_{m'k'} + \beta_{m'k'} \operatorname{tr}\left(\boldsymbol{\Phi}_{m'k}^{-1} \boldsymbol{R}_{m'k}\right)\right)^* & k' \in \mathscr{P}_k \\ 0, & k' \notin \mathscr{P}_k. \end{cases} \end{aligned} \tag{23}$$

that is simple in principle, low in complexity and easy to implement. However, it depends on the selection of the initial centre points. If the initial centre points are not selected properly, the performance of the system will degrade. Compared with the k-means algorithm, the hierarchical clustering algorithm [25] also has the characteristics of simplicity and easy implementation, but this algorithm does not rely on the selection of the initial centre points. Therefore, a hierarchical clustering algorithm is adopted in this paper.

The hierarchical clustering algorithm first assumes K users as K user clusters and then merges the clusters with the greatest channel similarity according to different link modes until they are merged to the desired number of clusters. The link mode is shown in Table 2. To reduce the computational complexity, we use a single chain as a measure of the distance between clusters.

In this paper, we consider users as points in space, describe each user by using the eigenmatrix of the channel covariance matrix corresponding to each user, and then use the Euclidean distance function to measure the channel similarity between every pair of users (clusters). The channel covariance matrix $\boldsymbol{COV}_k$ of the kth user and the channel similarity $d_c\left(\boldsymbol{U}_k, \boldsymbol{V}_g\right)$ between two users (clusters) are defined as

$$\boldsymbol{COV}_k = \mathrm{diag}\left(\boldsymbol{C}_{1k}, \ldots, \boldsymbol{C}_{Mk}\right), \tag{30}$$

$$d_c\left(\boldsymbol{U}_k, \boldsymbol{V}_g\right) = \left\|\boldsymbol{U}_k\boldsymbol{U}_k^H - \boldsymbol{V}_g\boldsymbol{V}_g^H\right\|_F^2, \tag{31}$$

where $\boldsymbol{COV}_k$ is the channel covariance matrix of the kth user and each element in the matrix can be calculated by formula (9). $\boldsymbol{U}_k$ is the eigenmatrix of the channel covariance matrix of the kth user. $\boldsymbol{V}_g$ is the eigenmatrix corresponding to the centre point of the gth user cluster. The smaller $d_c\left(\boldsymbol{U}_k, \boldsymbol{V}_g\right)$ is, the higher the similarity of the feature space matrix between two users (groups); that is, the higher the channel similarity between the two users (clusters) [27]. Based on the link definition and channel similarity measurement formula given, we propose a hierarchical clustering algorithm, as shown in Algorithm 2.

Algorithm 2 Hierarchical User Clustering Algorithm

Input: User set $U = \{1, 2, \cdots, K\}$, channel correlation matrix $\boldsymbol{COV}_k$,
number of clusters G
Output: Clustering results

1. Initialize each user as a cluster
2. for $k = 1, 2, 3, \ldots, K$
3. for $j = 1, 2, 3, \ldots, K$
4. Use formula (31) to calculate the similarity between two users (clusters)
5. end
6. end
7. While (Number of clusters $N1 >$ preset cluster number G)
8. Merge the two user clusters with the highest similarity
9. Recalculate the distance between the newly merged cluster and the other clusters according to the single linkage distance formula
10. end

B. ACCESS POINT SELECTION

Based on the LSFD coefficient of the optimization result in Section III and the user clustering result in Section IV-A, we propose a suboptimal access point selection algorithm.

The LSFD coefficient, which is the optimization result of the max-min optimization problem in Section III, can be used to evaluate the channel quality between the user and the AP [20]. If the signal received by the CPU contains a considerable amount of interference and noise, such interference and noise can be reduced by adjusting the LSFD coefficient. Therefore, we use the LSFD coefficient $\alpha_{m,k}$ as the AP selection criterion. However, the superiority of the system performance cannot be fully guaranteed by only this parameter. Analyzing the formula (20), SINR is inversely proportional to the channel estimation error. So we take the normalized channel estimation mean square error $\eta_{m,k}$ as another evaluation factor and use the $\eta_{m,k}$ to characterize the influence of the channel estimation error of the mth AP on the SINR. Based on the above analysis, we adopt the LSFD coefficient and the normalized channel estimation mean square error for the comprehensive evaluation of channel quality and AP selection, so as to ensure superior system performance. The AP selection parameter can be defined as

$$\Gamma_{mk} = \frac{\alpha_{mk}}{\eta_{mk}}, \tag{32}$$

and

$$\begin{aligned}\eta_{mk} &= \frac{\sum_{l=1}^{N} \mathrm{var}_{mlk}}{N\beta_{mk}} \\ &= \frac{\sum_{l=1}^{N}\left(\left(\beta_{mk} + \left[\bar{\boldsymbol{h}}_{mk}\right]_l^2\right) - \frac{\tau\rho_{\mathrm{p}}\left(\beta_{mk}+\left[\bar{\boldsymbol{h}}_{mk}\right]_l^2\right)^2}{\rho_p\tau\sum_{i\in\mathscr{P}_k}\left(\beta_{mi}+\left[\bar{\boldsymbol{h}}_{mi}\right]_l^2\right)+\sigma^2}\right)}{N\beta_{mk}},\end{aligned} \tag{33}$$

where var_{mlk} is the lth component of the channel estimation mean-squared error between the mth AP and kth user.

The proposed algorithm uses the user clustering method to reduce the number of AP selections and uses the AP selection coefficient to select the paths with good channel quality. Therefore, through the joint processing of user clustering and AP selection, the proposed algorithm reduces the pressure on the fronthaul link while taking into account the superiority of the system performance and the computational complexity. The specific process is shown in Algorithm 3.

C. COMPLEXITY AND CONVERGENCE ANALYSIS

1) COMPLEXITY ANALYSIS

The AP selection algorithm proposed in this paper is composed of three parts: Algorithm 1, Algorithm 2, and the AP selection parameter sort algorithm. In the first part of

Algorithm 3 Joint User Clustering and AP Selection Algorithm

1. Perform Algorithm 1.
2. Perform Algorithm 2. Get G user clusters. Randomly select a user in each user cluster as the central user.
3. Initialize the subset of APs that serve user g, g=1,2,3, . . . ,G, $M_g = \varnothing$.
4. Calculate the AP selection metric parameter Γ_{mk}, m=1,2,3, . . . ,M according to formula (32).
5. for i=1,2,3, . . . ,G
6. Sort the APs in descending order according to Γ_{mi}. Let W_i represent the descending set of APs, and let $W_i = \left\{Ap^1, \ldots, A\,p^M\right\}$.
7. Select the first L APs in set W_i and add them to set M_i
8. $d_{mi} = \begin{cases} 1 \text{ if } AP_m \in M_i \\ 0 \text{ if } AP_m \notin M_i \end{cases}$
9. All users in cluster i have the same AP selection matrix as user i
10. end
11. Insert the new $\mathbf{D}_k = \operatorname{diag}(d_{1\,k}, \ldots, d_{Mk})$ into (20) to obtain the SINR of the system.

the algorithm, we use the iterative optimization method to solve Algorithm 1. In each iteration of Algorithm 1, we use the bisection method to obtain a feasible solution to optimization problem (26) and then use the feasible solution obtained to calculate the value of $\boldsymbol{\alpha}_k$ in (29). the number of iterations needed for the bisection method is $\lceil \log_2 (t_{\text{ini}}/\epsilon) \rceil$. Within each iteration, the cost of solving the optimal power control coefficient is that of solving (26), which includes K variables and $2K$ constraints, so its complexity is $O\left(K^3\right)$ [28]; the complexity of solving the optimal LSFD coefficient is $O\left(|M_k|^2 K\right)$, and $|M_k|$ is the subset of APs serving user k. Therefore, the time complexity of Algorithm 1 is $O\left(\lceil \log_2 (t_{\text{ini}}/\epsilon) \rceil |M_k|^2 K^4\right)$. In the second part of the algorithm, the complexity of hierarchical clustering is $O\left(\text{K}^2 \log \text{K}\right)$. Based on Algorithm 1 and Algorithm 2, the third step is to calculate the access point selection parameters, sort the access point selection parameters of each cluster centre, and select the APs with the largest parameters to serve user k. At this stage, the complexity is $O\,(GM \log \text{M})$, where G is the number of user clusters.

2) CONVERGENCE ANALYSIS

Algorithm 1 is the first of the three components of Algorithm 3 and solves the joint optimization problem P in (24) through an iterative optimization method. The second component of Algorithm 3 uses hierarchical clustering to divide users into a preset number of clusters. The third component of Algorithm 3 is used to sort the access point selection coefficients and select APs with large coefficients to serve users. Since the second and third components have little influence on convergence analysis, the convergence of Algorithm 3 is determined by Algorithm 1. To determine the solution of the problem P in (24), we decompose Algorithm 1 into two subproblems related to power control coefficient and LSFD coefficient, both of which can be guaranteed to converge [22], [29]. Based on the convergence of these two subproblems, we consider the overall convergence of Algorithm 1. Let $f\left(p^{(i)}, \boldsymbol{\alpha}_k{}^{(i)}\right)$ be the minimum of the SINRs in problem P, obtained at the ith iteration. In the $(i+1)$ iteration, we have $f\left(p^{(i)}, \boldsymbol{\alpha}_k{}^{(i)}\right) \leq f\left(p^{(i+1)}, \boldsymbol{\alpha}_k{}^{(i)}\right)$, where $p^{(i+1)}$ are the updated power control coefficients obtained by solving problem P1 with fixed $\boldsymbol{\alpha}_k{}^{(i)}$. Additionally, by the non-decreasing of the objective function of problem P2, we can obtain $f\left(p^{(i+1)}, \boldsymbol{\alpha}_k{}^{(i)}\right) \leq f\left(p^{(i+1)}, \boldsymbol{\alpha}_k{}^{(i+1)}\right)$, where $\boldsymbol{\alpha}_k{}^{(i+1)}$ are the local LSFD coefficients achieved by solving problem P2 with fixed $p^{(i+1)}$. Therefore, after the $(i+1)$th iteration, we have $f\left(p^{(i)}, \boldsymbol{\alpha}_k{}^{(i)}\right) \leq f\left(p^{(i+1)}, \boldsymbol{\alpha}_k{}^{(i+1)}\right)$. Therefore, the objective function generated by Algorithm 1 is nondecreasing. Moreover, due to the power control coefficients and LSFD coefficients constraints, the objective function will converge to a local optimal value over iterations.

V. NUMERICAL RESULTS AND DISCUSSION

This section evaluates the performance of the proposed algorithm. One hundred APs equipped with $N = 20$ antennas and 40 users are uniformly distributed at random within a square of size $1 \times 1\,\text{km}^2$. Based on the 3GPP model in [30], the possibility of having an LOS component mainly depends on the distance d_{mk}, which is modeled as

$$\text{Possibility (LOS)} = \begin{cases} 1 - \dfrac{d_{mk}}{300}, & 0 < d_{mk} < 300\text{m}, \\ 0, & d_{mk} \geq 300\text{m}. \end{cases} \tag{34}$$

The Rician factor in (3) and (4) can be calculated as follows [31], [32]:

$$\kappa_{m,k} = \begin{cases} 10^{1.3-0.003 d_{mk}}, & \text{if an LOS path exists,} \\ 0, & \text{if an LOS path does not exist.} \end{cases} \tag{35}$$

For the path loss in (3) and (4), we use the COST 321 Walfisch–Ikegami model in [30]:

$$\text{PL}_{m,k} = \begin{cases} -30.18 - 26 \log_{10}\left(\dfrac{d_{mk}}{1\text{m}}\right) + F_{mk}, & k_{mk} \neq 0, \\ -34.53 - 38 \log_{10}\left(\dfrac{d_{mk}}{1\text{m}}\right) + F_{mk}, & k_{mk} = 0, \end{cases} \tag{36}$$

where the shadow fading coefficient is $F_{m,k} = \sqrt{\delta} a_m + \sqrt{1-\delta} b_k$. $a_m \sim \mathcal{N}\left(0, \sigma_{\text{sf}}^2\right)$ and $b_k \sim \mathcal{N}\left(0, \sigma_{\text{sf}}^2\right)$ are independent random variables. we choose the parameters summarized in Table 3.

Fig. 2 shows the distribution of a target user cluster and the selected access points under the proposed joint user cluster and access point selection algorithm. In Fig. 2, we use the red box "□" to mark users in the same cluster, and the green "○" to mark the APs selected by the user cluster. According to the theoretical analysis, the user needs to select the APs with the

TABLE 3. System parameters for the simulation.

Parameter	Value
Bandwidth	20MHz
Noise power	-90dBm
AP antenna height	12.5m
User antenna height	1.5m
ρ_p	200mW
σ_{sf},δ	8,0.5
τ_c,τ ,τ_u	200,10,190

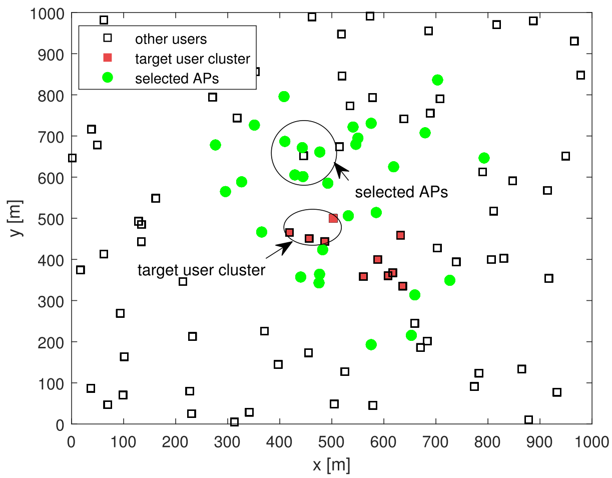

FIGURE 2. The distribution of a target user cluster and the selected access points.

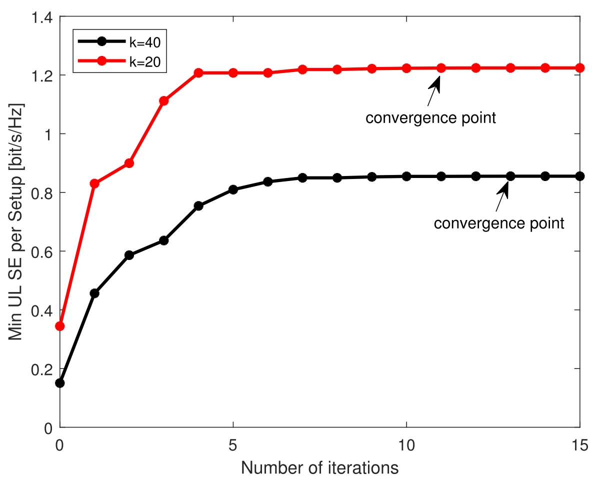

FIGURE 3. Min UL SE versus the number of iterations.

smallest noise and channel estimation error. It can be seen from the figure that most APs up to theoretical requirements are geographically close to the target user.

In Fig. 3, the minimum uplink spectral efficiency of all users in each setup is described as a function of the number of iterations, where the number of users is $k = 20$ and 40 and the number of access points is $M = 60$. Fig. 2 shows that the proposed algorithm converges very quickly and can converge to a stationary point within 15 iterations. We can also see that when the number of users is reduced from 40 to 20, the spectral efficiency of the stationary point increases by approximately 43%.

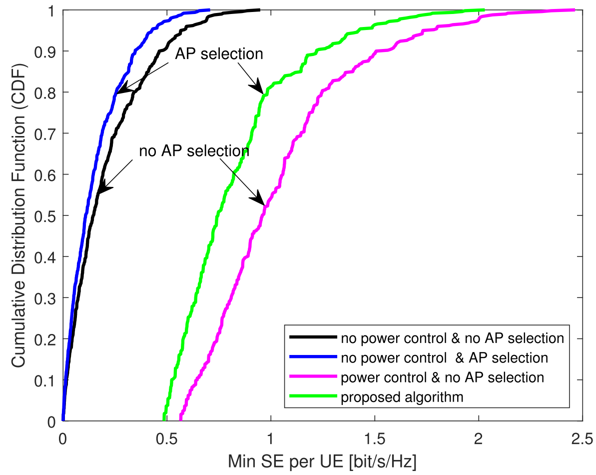

FIGURE 4. CDF of Min UL SE with/without power control and AP selection where M = 100, K = 40.

Fig. 4 shows the cumulative distribution of the minimum uplink spectral efficiency of each user for four cases: case 1, neither power control nor AP selection is used; case 2, AP selection is used but power control is not used; case 3, power control is used but AP selection is not used; and case 4, our proposed algorithm with power control, user clustering, and AP selection. According to the simulation results in Fig. 4, power and LSFD coefficient optimization improves the system performance. Compared with case 2 and our proposed algorithm, in terms of the 95% likely performance, the uplink minimum spectral efficiency improves by approximately 0.8 bit/s/Hz. The reason is that our proposed algorithm not only reduces the interference between users but also considers the fairness between users.

Fig. 5 shows the average minimum uplink spectral efficiency of the system under the same four cases as in Fig. 4. By observing the spectral efficiency of the system when $M = 40$, 60, 80, and 100, we can see that as the number of APs increases, the performance of the system improves. The reason is that as the number of APs increases, the probability of better-quality channels also increases. Through AP selection, users can choose a better transmission channel without increasing the interference between users.

To better demonstrate the performance, the AP selection scheme of this paper is compared with the other five AP selection schemes:

- AP selection based on the largest large-scale fading in [7]: In this algorithm, the AP with the largest large-scale fading is selected by the user. This strategy is denoted as 'Largest Large-Scale Fading [7]'.
- AP selection based on the effective channel gain in [12]: In this algorithm, the AP with the highest effective channel gain is selected. In [12], the effective channel gain is defined as the self-channel quality minus the sum of the other user interference. This algorithm is denoted as 'Largest Effective Channel Gain [12]'.

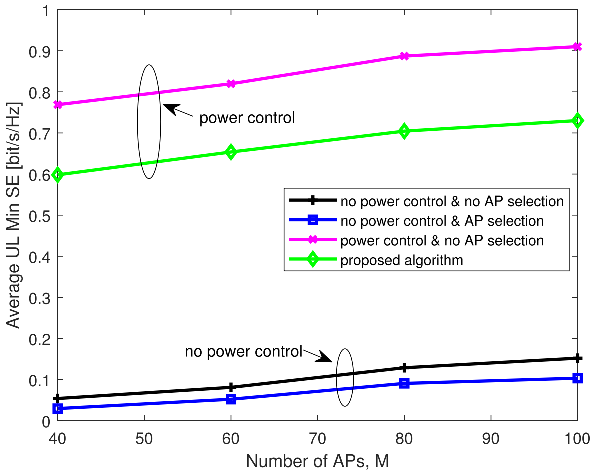

FIGURE 5. Average Min UL SE with/without power control and AP selection where M = 40,60,80,100, K = 40.

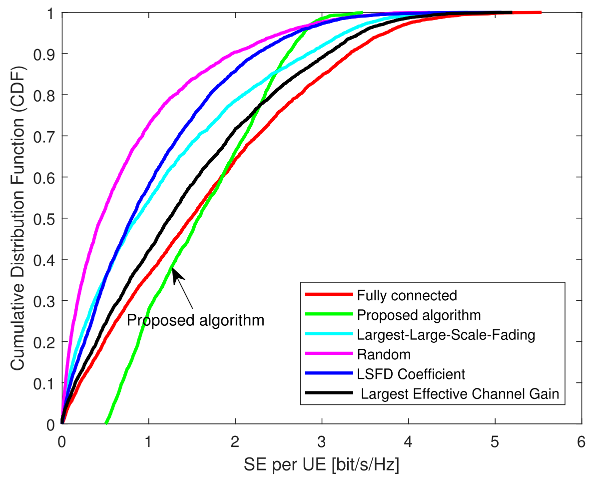

FIGURE 6. CDF of UL SE for the six AP selection schemes where M = 100, K = 40.

- AP selection based on the LSFD coefficient in [17]: In this algorithm, the user selects an AP with an LSFD coefficient greater than the threshold. This algorithm is denoted as 'LSFD Coefficient [17]'.
- Random algorithm: an AP is randomly assigned to users. Since some access points may not be able to provide services for any user, in the simulation, we ensure that each access point provides services for at least one user for comparison. This algorithm is denoted as "Random".
- Fully connected algorithm: The user does not select APs and can connect to all APs in the system. This algorithm is denoted as 'Fully connected'.

As shown in Fig. 6, the proposed algorithm is superior to the largest large-scale fading, largest effective channel gain, and LSFD coefficient algorithms in terms of the median performance. The median uplink SE of the proposed algorithm is approximately 1.58 bit/s/Hz, which is approximately 27% higher than that of the largest effective channel gain algorithm (1.24 bit/s/Hz) and almost twice that of the largest large-scale fading algorithm (0.8 bit/s/Hz). The reason is that the AP selection algorithms in [7], [12], [17] ignore the influence of the channel estimation error and power allocation on the channel quality. Therefore, our proposed scheme can more effectively and accurately select channels with better signal quality. The median uplink SE of the fully connected algorithm is very close to that of the proposed algorithm. In addition, it can be seen from the simulation result that according to our proposed algorithm, 90% of the average uplink SE of the fully connected algorithm can be reached by selecting approximately 50% of the APs. Although the SE is slightly reduced, the pressure on the fronthaul link is greatly reduced. The random scheme has the worst performance because the users connect to the AP randomly.

Fig. 7 shows the average uplink spectral efficiency of the system when users are clustered with different numbers. As shown in the figure, the more clusters there are, the higher the average SE of the system because more clusters mean that more users can obtain the suitable AP subset, which results in a better SE for the system. In the case of 40 users in 20 clusters, the spectral efficiency of the system can reach 90% of the value when they are not clustered. Despite the slightly reduced system performance, only 50% of the users need AP selection, which effectively reduces the fronthaul link pressure and computational complexity of the algorithm.

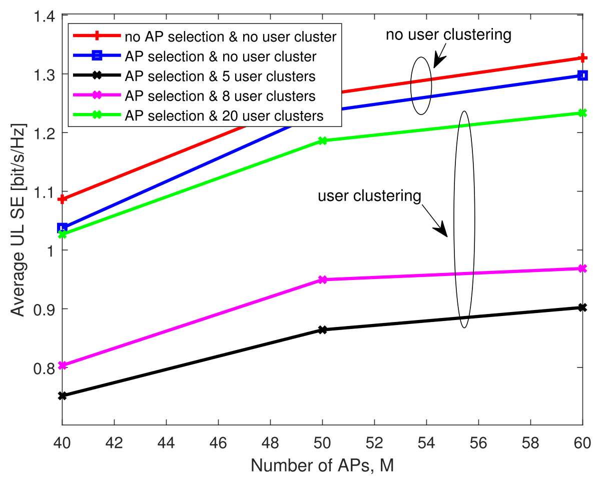

FIGURE 7. Average UL SE with/without user cluster for M = 40,50,60, K = 40.

Fig. 8 compares the bit error rate of the system under different AP selection algorithms. As shown in the figure, the proposed AP selection algorithm has the lowest bit error rate, the LSFD coefficient algorithm has the highest bit error rate, and the bit error rates of the largest large-scale fading and largest effective channel gain algorithms are between the above two. The reason why the bit error rate under the proposed algorithm is lower than that of the other three AP selection algorithms is that the proposed AP selection algorithm is based on the channel estimation accuracy. Therefore, the proposed AP selection algorithm has certain advantages in terms of the bit error rate.

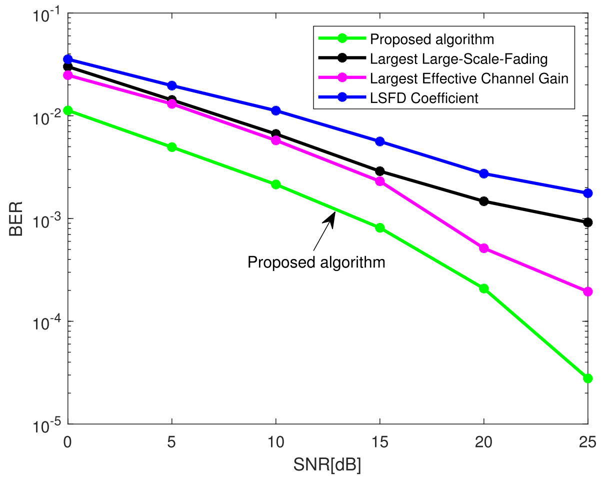

FIGURE 8. **The BER for the four AP selection schemes where M = 100, K = 40.**

VI. CONCLUSION

In this paper, we investigated the spectral efficiency of a limited-fronthaul cell-free massive MIMO system over a Rician fading channel, taking into account the effects of multiple-antenna AP selection, user clustering, channel estimation error, and power control. To reduce the pressure on the fronthaul, we first solved the problem of nonconvex optimization while maximizing the minimum system spectral efficiency through iterative optimization. Based on the optimization results, a joint user clustering and AP selection algorithm considering computational complexity and system performance was proposed. The simulation results showed that our proposed algorithm can improve the spectral efficiency and reduce the bit error rate of the system. In addition, the proposed algorithm required only approximately 50% of the APs to achieve 90% spectral efficiency without AP selection, and the pressure on the fronthaul could effectively be reduced, while the performance was only slightly reduced. In future research, we will extend our research from noncorrelated channels to correlated channels [33], [34]. Furthermore, we will analyze the performance of the limited-fronthaul cell-free massive MIMO system under spatially correlated Rician fading channels.

REFERENCES

[1] H. Q. Ngo, A. Ashikhmin, H. Yang, E. G. Larsson, and T. L. Marzetta, "Cell-free massive MIMO versus small cells," *IEEE Trans. Wireless Commun.*, vol. 16, no. 3, pp. 1834–1850, Mar. 2017.
[2] G. Interdonato, E. Björnson, H. Quoc Ngo, P. Frenger, and E. G. Larsson, "Ubiquitous cell-free massive MIMO communications," *EURASIP J. Wireless Commun. Netw.*, vol. 2019, no. 1, p. 197, Dec. 2019.
[3] T. C. Mai, H. Q. Ngo, and T. Q. Duong, "Downlink spectral efficiency of cell-free massive MIMO systems with multi-antenna users," *IEEE Trans. Commun.*, vol. 68, no. 8, pp. 4803–4815, Aug. 2020.
[4] G. Femenias and F. Riera-Palou, "Fronthaul-constrained cell-free massive MIMO with low resolution ADCs," *IEEE Access*, vol. 8, pp. 116195–116215, 2020.
[5] M. Bashar, K. Cumanan, A. G. Burr, H. Q. Ngo, E. G. Larsson, and P. Xiao, "Energy efficiency of the cell-free massive MIMO uplink with optimal uniform quantization," *IEEE Trans. Green Commun. Netw.*, vol. 3, no. 4, pp. 971–987, Dec. 2019.
[6] M. Bashar, H. Q. Ngo, A. G. Burr, D. Maryopi, K. Cumanan, and E. G. Larsson, "On the performance of backhaul constrained cell-free massive MIMO with linear receivers," in *Proc. 52nd Asilomar Conf. Signals, Syst., Comput.*, Oct. 2018, pp. 624–628.
[7] H. Q. Ngo, L.-N. Tran, T. Q. Duong, M. Matthaiou, and E. G. Larsson, "On the total energy efficiency of cell-free massive MIMO," *IEEE Trans. Green Commun. Netw.*, vol. 2, no. 1, pp. 25–39, Mar. 2018.
[8] M. Bashar, K. Cumanan, A. G. Burr, H. Q. Ngo, and M. Debbah, "Cell-free massive MIMO with limited backhaul," in *Proc. IEEE Int. Conf. Commun. (ICC)*, May 2018, pp. 1–7.
[9] J. Zhang, Y. Wei, E. Björnson, Y. Han, and X. Li, "Spectral and energy efficiency of cell-free massive MIMO systems with hardware impairments," in *Proc. 9th Int. Conf. Wireless Commun. Signal Process. (WCSP)*, Oct. 2017, pp. 1–6.
[10] E. Björnson and L. Sanguinetti, "Scalable cell-free massive MIMO systems," *IEEE Trans. Commun.*, vol. 68, no. 7, pp. 4247–4261, Jul. 2020.
[11] T. H. Nguyen, T. K. Nguyen, H. D. Han, and V. D. Nguyen, "Optimal power control and load balancing for uplink cell-free multi-user massive MIMO," *IEEE Access*, vol. 6, pp. 14462–14473, 2018.
[12] H. T. Dao and S. Kim, "Effective channel gain-based access point selection in cell-free massive MIMO systems," *IEEE Access*, vol. 8, pp. 108127–108132, 2020.
[13] M. N. Boroujerdi, A. Abbasfar, and M. Ghanbari, "Antenna assignment in cell free massive MIMO systems," in *Proc. Iranian Conf. Electr. Eng. (ICEE)*, May 2017, pp. 1747–1751.
[14] T. X. Vu, S. Chatzinotas, S. ShahbazPanahi, and B. Ottersten, "Joint power allocation and access point selection for cell-free massive MIMO," in *Proc. IEEE Int. Conf. Commun. (ICC)*, Jun. 2020, pp. 1–6.
[15] T. Van Chien, E. Björnson, and E. G. Larsson, "Joint power allocation and load balancing optimization for energy-efficient cell-free massive MIMO networks," *IEEE Trans. Wireless Commun.*, vol. 19, no. 10, pp. 6798–6812, Oct. 2020.
[16] G. Dong, H. Zhang, S. Jin, and D. Yuan, "Energy-efficiency-oriented joint user association and power allocation in distributed massive MIMO systems," *IEEE Trans. Veh. Technol.*, vol. 68, no. 6, pp. 5794–5808, Jun. 2019.
[17] H. Q. Ngo, H. Tataria, M. Matthaiou, S. Jin, and E. G. Larsson, "On the performance of cell-free massive MIMO in Ricean fading," in *Proc. 52nd Asilomar Conf. Signals, Syst., Comput.*, Oct. 2018, pp. 980–984.
[18] Ö. Özdogan, E. Björnson, and E. G. Larsson, "Uplink spectral efficiency of massive MIMO with spatially correlated rician fading," in *Proc. IEEE 19th Int. Workshop Signal Process. Adv. Wireless Commun. (SPAWC)*, Jun. 2018, pp. 1–5.
[19] T. K. Nguyen and T. H. Nguyen, "Performance of assigning pilot sequences in cell free massive MIMO under SINR constraints," in *Proc. IEEE 7th Int. Conf. Commun. Electron. (ICCE)*, Jul. 2018, pp. 121–126.
[20] Ö. Özdogan, E. Björnson, and J. Zhang, "Performance of cell-free massive MIMO with Rician fading and phase shifts," *IEEE Trans. Wireless Commun.*, vol. 18, no. 11, pp. 5299–5315, Nov. 2019.
[21] T. Van Chien, C. Mollén, and E. Björnson, "Large-scale-fading decoding in cellular massive MIMO systems with spatially correlated channels," *IEEE Trans. Commun.*, vol. 67, no. 4, pp. 2746–2762, Apr. 2019.
[22] E. Björnson, J. Hoydis, and L. Sanguinetti, "Massive MIMO networks: Spectral, energy, and hardware efficiency," *Found. Trends Signal Process.*, vol. 11, nos. 3–4, pp. 154–655, 2017.
[23] S. Buzzi and C. D'Andrea, "Cell-free massive MIMO: User-centric approach," *IEEE Wireless Commun. Lett.*, vol. 6, no. 6, pp. 706–709, Dec. 2017.
[24] Y. Sun, S. Lv, S. Liu, and Y. Zhang, "Density based user grouping for massive MIMO downlink in FDD system," in *Proc. IEEE 9th Int. Conf. Commun. Softw. Netw. (ICCSN)*, May 2017, pp. 448–453.
[25] S. Zhou, Z. Xu, and F. Liu, "Method for determining the optimal number of clusters based on agglomerative hierarchical clustering," *IEEE Trans. Neural Netw. Learn. Syst.*, vol. 28, no. 12, pp. 3007–3017, Dec. 2017.
[26] Y. Xu, G. Yue, and S. Mao, "User grouping for massive MIMO in FDD systems: New design methods and analysis," *IEEE Access*, vol. 2, pp. 947–959, 2014.
[27] Y. Xie, B. Li, J. Fan, X. Zhou, G. Y. Li, and X. Li, "User grouping with load balance in FDD massive MIMO systems," in *Proc. IEEE 86th Veh. Technol. Conf. (VTC-Fall)*, Sep. 2017, pp. 1–6.
[28] S. Boyd and L. Vandenberghe, *Convex Optimization*. Cambrige, U.K.: Cambrige Univ. Press, 2004.
[29] N. A. Rahim, A. Amir, A. Amir, and J. Selvaraj, "Application of bisection search method for maximum power extraction," in *Proc. Int. Conf. Intell. Adv. Syst. (ICIAS)*, Aug. 2018, pp. 1–4.

[30] *Spatial Channel Model for Multiple Input Multiple Output (MIMO) Simulations*, document TR25.996 (V14.0.0), 3GPP, 2017.
[31] Ö. Özdogan, E. Björnson, and J. Zhang, "Cell-free massive MIMO with Rician fading: Estimation schemes and spectral efficiency," in *Proc. 52nd Asilomar Conf. Signals, Syst., Comput.*, Oct. 2018, pp. 975–979.
[32] Ö. Özdogan, E. Björnson, and E. G. Larsson, "Massive MIMO with spatially correlated Rician fading channels," *IEEE Trans. Commun.*, vol. 67, no. 5, pp. 3234–3250, May 2019.
[33] M. Ke, Z. Gao, Y. Wu, X. Gao, and K.-K. Wong, "Massive access in cell-free massive MIMO-based Internet of Things: Cloud computing and edge computing paradigms," *IEEE J. Sel. Areas Commun.*, early access, Aug. 24, 2020, doi: 10.1109/JSAC.2020.3018807.
[34] M. Ke, Z. Gao, Y. Wu, X. Gao, and R. Schober, "Compressive sensing-based adaptive active user detection and channel estimation: Massive access meets massive MIMO," *IEEE Trans. Signal Process.*, vol. 68, pp. 764–779, 2020.

RUI WANG is currently pursuing the Ph.D. degree with the Key Laboratory of New Generation Broadband Mobile Communication Technology, Chongqing University of Posts and Telecommunications, Chongqing, China. She is also with Yuxi Normal University, Yunnan, China. Her research interests include resource allocation, dynamic cooperation, and precoding for cell-free massive MIMO communications.

MIN SHEN received the B.S. degree from the Chongqing University of Posts and Telecommunications (CQUPT), China, in 1985, and the M.S. degree from the Beijing University of Posts and Telecommunications, China, in 1992. She is currently a Professor with the School of Communication and Information Engineering, CQUPT. Her primary research interests include wireless communications technology and signal processing, and their applications in wireless networks and related fields.

YUN HE (Graduate Student Member, IEEE) received the B.E. and M.E. degrees from the Chongqing University of Posts and Telecommunications, China, in 2008 and 2012, respectively. She is currently pursuing the Ph.D. degree with the Department of Communication and Information Engineering, Chongqing University of Posts and Telecommunications. Her research interests include the next-generation mobile communications, communication theory, and signal processing. In the context of wireless communications, her interests include collaborative communications, MIMO systems, and energy efficiency optimization.

XIANGYAN LIU received the B.Eng. and M.Eng. degrees from the Chengdu University of Technology, China, in 2014 and 2017, respectively. She is currently pursuing the Ph.D. degree with the Chongqing University of Posts and Telecommunications, China. Her main research interests include resource allocation, mobile edge computing, and device-to-device communications.